ELSEVIER

Journal of Molecular Catalysis A: Chemical 158 (2000) 19–35

JOURNAL OF MOLECULAR CATALYSIS A: CHEMICAL

www.elsevier.com/locate/molcata

^{1}H NMR and EPR spectroscopic monitoring of the reactive intermediates of (Salen)Mn^{III} catalyzed olefin epoxidation

Konstantin P. Bryliakov [a], Dmitrii E. Babushkin [b], Evgenii P. Talsi [b,*]

[a] *Natural Science Department, Novosibirsk State University, 630090 Novosibirsk, Russia*
[b] *Boreskov Institute of Catalysis, Pr. Akademika Lavrentieva 5, 630090 Novosibirsk, Russia*

Abstract

Using ^{1}H NMR and EPR spectroscopy, manganese species formed in the catalytic systems **1** + iodosobenzene (PhIO) and **1** + meta-chloroperoxybenzoic acid (*m*-CPBA), where **1** is (*R,R*)-(−)-*N,N′*-bis(3,5-di-*tert*-butylsalicylidene)-1,2-cyclohexanediamino-manganese(III) chloride ([(Salen)Mn^{III}]) were studied. Three types of manganese complexes were characterized in the catalytic system **1** + PhIO (**4**–**6**). Complex **4** is very unstable and reacts with styrene at −20°C to afford styrene oxide. It exhibits three signals of *t*Bu groups at 1.68, 1.64 and 1.42 ppm. This pattern closely resembles that for a model complex [(Salen)Mn^{V} ≡ N]. Based on these data, **4** was identified as d^2 low-spin oxomanganese(V) complex [(Salen)Mn^{V} = O]$^+$. Complexes **5** and **6** are relatively stable at −20°C and poorly reactive towards styrene at this temperature. They display ^{1}H NMR spectra characteristic for antiferromagnetically coupled μ-oxo-dinuclear Mn^{IV} species and are identified as dinuclear complexes [(Salen)LMn^{IV}-*O*-Mn^{IV}(Salen)L′] with L, L′ = Cl$^-$ and PhIO. It was found by EPR that the acylperoxo complex (Salen)Mn^{III}(OOCOAr) (**7**) was formed at the first stage of the interaction of **1** with *m*-CPBA in CH_2Cl_2. Complex **7** is unstable and converts into manganese(IV) oxo complex [(Salen)Mn^{IV}(O)] (**8**). The evaluated first order rate constant of this conversion is 0.25 ± 0.08 min^{-1} at −70°C. Complex **7** reacts with styrene with the rate constant 1.1 ± 0.4 M^{-1} min^{-1} at −70°C to give epoxide and restore **1**. Complex **8** is inert towards styrene at low temperature. The effect of donor ligand *N*-methylmorpholine-*N*-oxide (NMO) on the epoxidation of styrene by the system **1** + *m*-CPBA was studied. Addition of NMO (2–5 equiv.) to the solution of **1** in CH_2Cl_2 before interaction with *m*-CPBA was found to dramatically increase the rate of undesirable transformation of the reactive acylperoxo complex **7**-NMO into relatively inert oxo complex-**8**-NMO. However, in the presence of styrene, such undesirable conversion is entirely suppressed by very rapid reaction of **8**-NMO with styrene to afford styrene oxide and restore **1**-NMO.

Keywords: Enantioselective epoxidation; Mechanism; Manganese salen complexes; EPR; ^{1}H NMR spectroscopy

1. Introduction

A recent major advance in catalytic enantioselective oxidation has been the epoxidation of prochiral unfunctionalized olefins catalyzed by chiral (Salen)Mn^{III} complexes [1–7]. The practically

* Corresponding author. Tel.: +7-383-235-5750; fax: +7-383-234-3766.
E-mail address: talsi@catalysis.nsk.su (E.P. Talsi).

1381-1169/00/$ - see front matter
PII: S1381-1169(00)00040-6

important catalytic system for enantioselective synthesis of *cis*-epoxides from Z-alkenes involves a two phase system with an aqueous buffered commercial bleach phase and the organic phase composed of a solution of substrate and catalyst in a suitable solvent [1]. Another perspective system consists of the combination of *m*-chloroperbenzoic acid (*m*-CPBA), *N*-methylmorpholine-*N*-oxide (NMO) and a catalyst in dichloromethane at low temperature (−78°C) [6,7]. The latter system is effective for the enantioselective epoxidation of styrene.

To elucidate the mechanism of (Salen)Mn^{III} catalyzed epoxidations, it is necessary to monitor the structure of the catalyst in the course of catalytic reaction. However, such data are very restricted. The observed enantioselelectivities were explained by models based on a reactive oxomanganese(V) species. Nevertheless, in none of that cases was the reactive species isolated or characterized. Only recently direct evidence for its existence has been obtained by electrospray tandem mass spectrometry [8]. However, it is still unclear whether the detected $[(Salen)Mn^{V}=O]^{+}$ intermediate really exists in detectable amount in the catalytic system studied ((Salen)Mn^{III} + PhIO) or it is formed in the course of MS experiment via fragmentation of μ-oxo dimeric complex $[(Salen)Mn^{IV}\text{-}O\text{-}Mn^{IV}(Salen)]^{+2}$ that is also present in the reaction mixture. For the catalytic system (Salen)Mn^{III} + *m*-CPBA an acylperoxo complex (Salen)Mn^{III}(OOCOAr) can be considered as an alternative reactive species. This year Groves and co-workers reported ^{1}H NMR characterization of oxomanganese(V) porphyrin [9].

In this work, we have undertaken studies of (Salen)Mn^{III} + PhIO, (Salen)Mn^{III} + *m*-CPBA and (Salen)Mn^{III} + *m*-CPBA + NMO catalytic systems using ^{1}H NMR and EPR spectroscopy. The main purpose was to characterize reactive intermediates of enantioselective epoxidation. ((*R*,*R*)-(−)-*N*,*N*′-bis(3,5-di-*tert*-butylsalicylidene)-1,2-cyclohexanediamino-manganese(III) chloride ([(Salen)Mn^{III}])(**1**)) was used as a catalyst. To assign EPR and ^{1}H NMR resonances of complex **1**, they were compared with those of the complexes N,*N*′-bis(salicylidene)ethylenediaminomanganese(III)chloride (**2**) and N,*N*′-bis(3,4,5,6-tetra-deutero-salicylidene)-1,2-cyclohexanediaminomanganese(III) chloride (**3**).

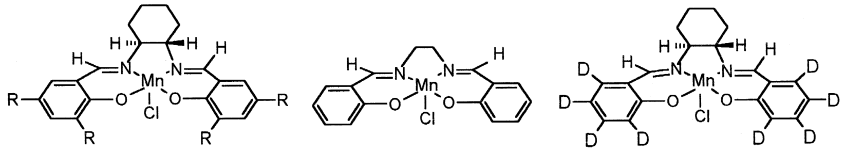

1 R = t-Bu 2 3

2. Experimental

2.1. General

((*R*,*R*)-(−)-*N*,*N*′-bis(3,5-di-*tert*-butyl-salicylidene)-1,2-cyclohexanediaminomanganese(III) chloride) (**1**), *N*,*N*′-bis(3,5-di-*tert*-butyl-salicylidene)-1,2-cyclohexanediamine, meta-chloroperoxybenzoic acid (*m*-CPBA), *N*-methylmorpholine *N*-oxide (NMO), $CDCl_3$, d_6-phenol and CD_2Cl_2 were purchased from Aldrich Chemical and were used as received. Iodosylbenzene was prepared by hydrolysis of (diacetoxyiodo)benzene (Aldrich) with 3 N aqueous sodium hydroxide and stored at 253 K. Complex **2** (*N*,*N*′-bis(salicylidene)ethylenediaminomanganese(III) chloride) and its Mn(II) precursor

were prepared as in Ref. [10]. Nitridomanganese(V) model complex [(Salen)$Mn^{V} \equiv N$] (Salen is (*R,R*)-(−)-*N,N′*-bis(3,5-di-*tert*-butyl-salicylidene)-1,2-cyclohexanediamine) was synthesized according to procedure described in Ref. [11]. (*R,R*)-(−)-*N,N′*-bis(3,4,5,6-tetra-deutero-salicylidene)-1,2-cyclohexanediamine (**3**) was prepared from d_6-phenol according to procedures described in Refs. [12] and [13]. All other chemicals and solvents were reagent grade and used without further purification.

2.2. Preparation of samples for EPR and ^{1}H NMR measurements

To study the reaction of **1** with *m*-CPBA and styrene at −90–0°C, the glass tube ($d = 3$ mm, $l = 200$ mm) with 0.2 ml of the solution of *m*-CPBA in CH_2Cl_2 (CD_2Cl_2) was placed into the quartz tube ($d = 5$ mm, $l = 150$ mm) containing 0.2 ml of the solution of **1** in CH_2Cl_2 or CD_2Cl_2 with additives of Py, NMO or styrene. These two tubes were immersed into a toluene bath at −90–0°C and stored for 5–10 min. To start the reaction, a preliminary weakened bottom of the glass tube was broken and two solutions were thoroughly mixed by inner tube as a mixer. In the appropriate moment of time after onset of reaction, the quartz tube was removed from the bath and frozen by immersion into liquid nitrogen. Then EPR and ^{1}H NMR spectra of this sample were recorded at the appropriate temperature. To study the reaction of **1** with PhIO, the solution of **1** in CH_2Cl_2(CD_2Cl_2) or $CDCl_3$ was shaken during 30 s–3 min at appropriate temperature with PhIO directly in NMR or EPR tube and then EPR and ^{1}H NMR spectra of the solution were recorded.

2.3. General procedure for the reactivity studies

The reactivities of the intermediate Mn^{III} and Mn^{IV} species towards styrene were determined by monitoring the intensities of the corresponding EPR signals after addition of styrene. The yield of the oxidation products (with respect to styrene unless other is outlined) was determined by GC, with enantiomeric excess determined by ^{1}H NMR spectroscopy. The chiral shift reagent tris(3-heptafluoropropyl-hydroxymethylene-(+)-camphorato) europium(III) derivative from Aldrich Chem. was used for ee measurements. Prior to the ^{1}H NMR study the oxidation products were isolated from the reaction mixture by evaporating in vacuo. The general epoxidation procedure for **1** + *m*-CPBA and **1** + *m*-CPBA + NMO catalytic systems was as in Ref. [7] (10 mol% of catalyst). For the epoxidation by **1** + PhIO catalytic system, 1 equiv. of PhIO powder was added to the mixture containing 0.2 M of styrene in CH_2Cl_2 and 0.02 M of catalyst at 0°C. The reaction mixture was stirred for 1h. The yield was 60%, ee 35%.

2.4. EPR and ^{1}H NMR measurements

EPR spectra (−196°C) were recorded at 9.2–9.3 GHz on a Bruker ER-200D X-band spectrometer. Measurements were made in quartz dewar with liquid nitrogen. The dual EPR cavity furnished with the spectrometer was used. Periclase crystal (MgO) with impurities of Mn^{2+} and Cr^{3+}, which served as a side reference, was placed into the center of the second compartment of the dual cavity.

The ^{1}H NMR spectra were recorded at 400.13 MHz using pulsed FT-NMR technique on a Bruker MSL-400 NMR spectrometer. Deuterated solvents were used to prepare the samples for the ^{1}H NMR studies. The following operating conditions were used: sweep width 50 000–500 000 Hz; spectrum accumulation frequency 5–10 Hz; number of scans 500–10 000. The data were accumulated with 16 K data point in the time domain and transformed with optimal exponential multiplication 1–20 Hz. Chemical shifts were calculated in parts per million (ppm) with positive values in the low field

direction with respect to internal reference TMS. The error in measuring the chemical shift values was ± 2 ppm for the line width around 4 kHz.

3. Results and discussion

3.1. Characterization of the initial complex **1**

3.1.1. Electron paramagnetic resonance

EPR spectroscopy has rarely been applied to study the electronic structure of trivalent manganese complexes. This is a result of the assumption that the non-Kramers spin states of such systems would be EPR silent, as a result of either large zero-field splittings or fast spin relaxation processes. Although a few EPR studies of trivalent manganese impurity ions and complexes have been reported, these have relied largely on indirect detection methods or very high observation frequencies [14–16]. There is the only report where weak EPR transition $g \approx 8$ was observed for Mn(III)tris(acetylacetonate) at 12 K by conventional X-band EPR spectroscopy [17]. The authors interpreted the Mn^{3+} spectrum using the following spin Hamiltonian:

$$H = \beta\left(g_x H_x S_x + g_y H_y S_y + g_z H_z S_z\right) + D\left(S_z^2 - 2\right) + E\left(S_x^2 - S_y^2\right) \quad (1)$$

The zero-field interaction splits the levels of an $S = 2$ spin system into two doublets, one comprised of linear combination of the $m_s = |\pm 2\rangle$ states and the other of the $m_s = |\pm 1\rangle$ states, and singlet corresponding to the $m_s = |0\rangle$ state. The forbidden EPR transitions may be observed between the levels of the $|\pm 2\rangle$ non-Kramers doublet.

The X-band EPR spectrum of a frozen 0.1 M solution of complex **1** in CH_2Cl_2 at -196°C is shown in Fig.1a. The field position and shape of the weak signal at $g = 7.8 \pm 0.3$ are close to those for the signal observed for Mn(III)tris(acetyacetonate) and attributed to forbidden transitions within non-Kramers doublet [17]. The relatively sharp resonance at $g = 4.3$ is characteristic of rhombic complexes of Fe(III) and belongs to very small admixtures (less than 1 mol%) of Fe(III) species in complex **1**. The addition of $FeCl_3 \cdot 6H_2O$ to the solution of complex **1** gives rise to sharp increase of the signal at $g = 4.3$. The Fe(III) impurities were detected not only in our particular sample. The EPR spectrum of optical isomer of complex **1** ((*S*,*S*)-(+)-*N*,*N*′-bis(3,5-di-*tert*-butyl-salicylidene)-1,2-cyclohexanediaminomanganese(III) chloride)**(1′)** (Aldrich) also displayed the resonance at $g = 4.3$ but its intensity was lower than that in complex **1** by a factor of two. The signals at g = 7.8 for complexes **1** and **1′** coincided. It is worth noting, that complexes **1** and **1′** display additional low field signal at $g \approx 12$ marked in Fig.1a with asterisk. This signal disappears in the presence of donor molecules such as Py, NMO, DMSO, MeOH and styrene. The nature of this signal is still unclear. We have compared EPR signals of 0.1 M solutions of complexes **1** and **2** in dimethylsulfoxide at -196°C. DMSO was used as a solvent due to proper solubility of both complexes. On assumption that the signal at $g = 7.8$ belongs to Mn(III), it is natural to expect that these signals would be similar for complexes **1** and **2** due to similarity in their structures. Indeed, the positions, shapes and intensities of the observed signals at $g = 7.8$ for complexes **1** and **2** coincided with accuracy of our experiment. This result supports the assignment of the resonance at $g = 7.8$ to complex **1**, but not to any manganese admixtures. It is improbable, that the concentrations of such admixtures would be the same in complexes **1** and **2**.

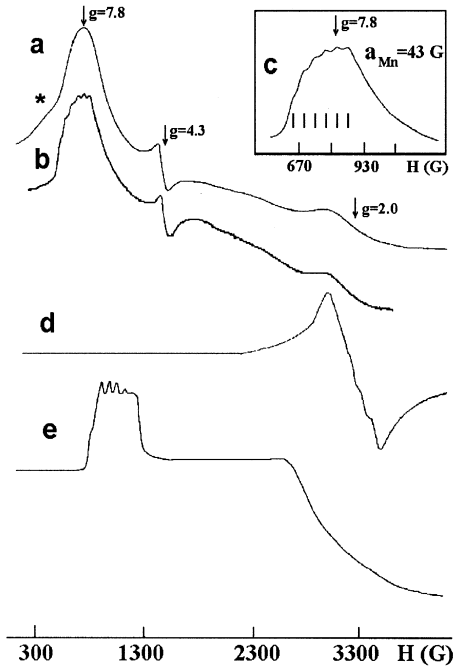

Fig. 1. X-band EPR spectra (−196°C) of 0.05 M solutions of complex **1** in CH_2Cl_2 (a) and in CH_2Cl_2, containing *N*-methylmorfoline-*N*-oxide ([NMO] = 1M) (b–c). EPR spectrum (−196°C) of (Salen)Mn^{II} precursor of complex **2** in DMSO (d). EPR spectrum (−196°C) of (Salen)Mn^{IV} complexes recorded 1 min after onset of reaction of complex **1** with one equivalent of *m*-cloroperbenzoic acid at 0°C (e). Spectrometer settings: frequency 9.3 GHz, microwave power 40 mW, modulation frequency 100 kHz, modulation amplitude 20G; gain 2.5×10^5 (a–c), 2.5×10^3 (d), 2.5×10^4 (e).

Coordination of NMO to complex **1** changes the shape of the EPR spectrum. The signal at $g \approx 12$ disappears and signal at $g = 7.8$ displays six-line hyperfine structure from one manganese ion ($I = 5/2$) (Fig. 1b–c). The hyperfine splitting ($A = 44 \pm 3$ G) that appears at the $g = 7.8$ signal is rather close to that determined for Mn(III) impurity ions in TiO_2 ($A_z = 53$ G) [15] and for Mn(III)tris(acetylacetonate) ($A_z = 55$ G) [17].

Mn(II) species ($S = 5/2$), which may be present as impurities in Mn(III) preparations, can also give rise to EPR features at low field. The two species can be clearly distinguished, however, because the $S = 5/2$ (Salen)Mn^{II} system produces very intense resonance at $g = 2$ in addition to any other features at low field. Fig.1d shows the EPR spectrum of (Salen)Mn^{II} precursor of complex **2** in DMSO prepared according to the procedure described in Ref. [9]. This spectrum was recorded with an amplification lower than that in Fig.1a by two orders of magnitude. It is seen that (Salen)Mn^{II} exhibits the intense signal at $g = 2$ with the partially resolved hyperfine splitting ($A = 87$ G) from manganese nucleus.

The (Salen)Mn^{IV} complexes obtained via reaction of complex **1** with one equivalent of *m*-CPBA in CH_2Cl_2 at 0°C exhibit a resonance at $g = 5.4 \pm 0.3$ with the hyperfine structure (hfs) ($A = 73$ G) typical for Mn(IV) species with $D > h\nu$ [18–21] (Fig.1e). The structure of these (Salen)Mn^{IV} complexes will be discussed in Section 3.3. The amplification in Fig. 1e is lower than that in Fig. 1a by one order of magnitude, while concentrations of Mn(III) and Mn(IV) species are equal. Thus, the signal of (Salen)Mn^{III} is much weaker than that of (Salen)Mn^{IV} at equal manganese concentrations. This result is in agreement with literature data. It was found for manganese impurity ions in TiO_2, that the resonance of Mn(III) is about an order of magnitude weaker than that of the same quantity of

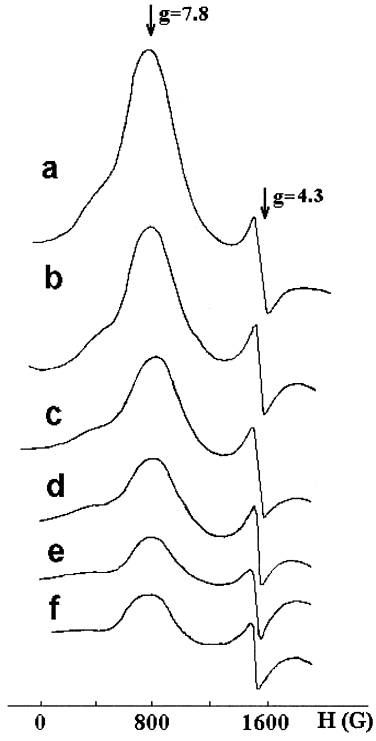

Fig. 2. X-band EPR spectra (−196°C) of 0.05 M solution of complex **1** in CH_2Cl_2 (a), and in CH_2Cl_2 containing various amounts of Py (b–f): [Py] = 0.0125 M (b), 0.025 M (c), 0.0375 M (d), 0.05 M (e), 0.1M (f). Gain 2.5×10^5 (a–e).

corresponding Mn(IV) species [16]. Based on the aforesaid, we can conclude that it is mononuclear (Salen)Mn^{III} complex **1** that exhibits EPR signal at $g = 7.8 \pm 0.3$. Dimers or higher aggregates of **1** can be ruled out. Based on the data for Mn^{III}/Mn^{IV} and Mn^{II}/Mn^{III} mixed-valence binuclear complexes, more than six line hyperfine splitting is expected for oligonuclear species [22,23].

The EPR signal of complex **1** was found to be very sensitive to the nature of axial ligands (compare Fig. 1a–b). Another illustration of this fact is presented in Fig. 2. It is seen that the intensity and shape of the resonance at $g = 7.8$ dramatically changed with an increase in the concentration of pyridine in the solution of complex **1**. This change discontinued when the [Py]/[**1**] ratio reached unity, in agreement with the coordination of one Py molecule per molecule of complex **1**. The reason for the decrease of the EPR signal of complex **1** via pyridine coordination is still unclear. It is known that the axial ligands dramatically affect the *D* value in Mn(III) porfirazine complexes [17]. Unfortunately, we have not found the relations between the value of D and probability of $|-2\rangle \rightarrow |+2\rangle$ transition in the literature. However, the sensitivity of EPR signal of complex **1** to axial ligation is useful for monitoring the composition of its coordination sphere.

In conclusion, (Salen)Mn^{III} complexes display rather characteristic signal at $g = 7.8$ in X-band EPR spectra, and can be clearly distinguished from (Salen)Mn^{II} and (Salen)Mn^{IV} species. This signal is sensitive to the nature of axial ligands of manganese.

3.1.2. Nuclear magnetic resonance

High-spin Mn(III), in octahedral field, has an ^5E electronic ground state and is expected to show well resolved isotropically shifted ^1H NMR spectra arising from ligand protons [24]. ^1H NMR

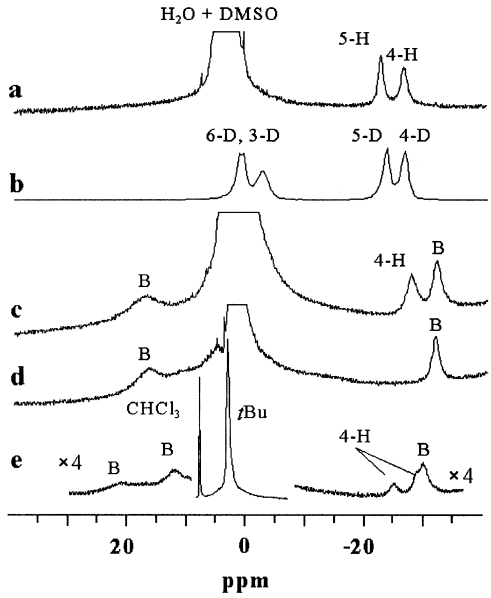

Fig. 3. ^{1}H NMR spectra (d_6-DMSO, 20°C) of **2** (a), **1** (c) and **3** (d). ^{2}D NMR spectrum (DMSO, 20°C) of **3** (b). ^{1}H NMR spectrum of **1** in $CDCl_3$ at −20°C (e). Concentration of complexes was 0.03 M. The spectra were recorded in the range +40 to −40 ppm.

spectrum of complex **2** in d_6-DMSO at 20°C is shown in Fig. 3a. The resonances at −22.2 ppm ($\Delta\omega_{1/2} = 450$ Hz) and −26.0 ppm ($\Delta\omega_{1/2} = 500$ Hz) were previously unambiguously assigned to 5th and 4th protons of aromatic rings of complex **2**, respectively [25]. We have additionally observed the resonance at −125 ppm ($\Delta\omega_{1/2} = 4$ kHz) assigned to two protons of ethylene bridge of complex **2** and very broad resonance at −405 ppm ($\Delta\omega_{1/2} = 10$ kHz) attributed to its imine protons (Fig. 4). The latter signal can be detected for complexes **1**, **2** and **3** at approximately the same field position. The resonances of 3rd and 6th protons of aromatic rings of complex **2** are masked in Fig. 3a by those of residual undeuterated water and DMSO. The ^{2}D NMR spectrum of complex **3** (Fig. 3b) shows, that the 3rd and 6th deuterons (and thus protons) of complex **3** display resonances at −1.9 and 2.0 ppm.

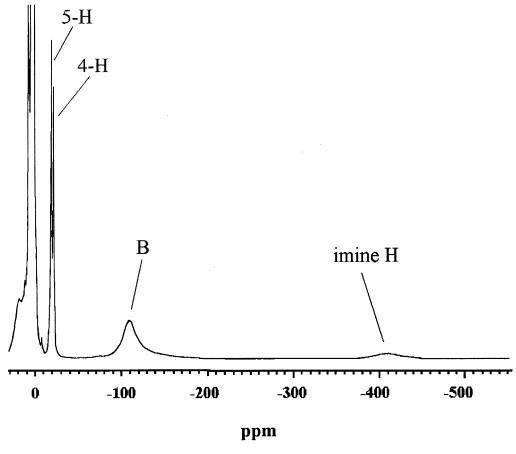

Fig. 4. ^{1}H NMR spectrum of 0.03 M solution of complex **2** in d-DMSO at 60°C. Letter B denotes the signal of two protons of the ethylene bridge. The spectrum was recorded in the range +30 to −500 ppm.

Thus, the 3rd and 6th protons of complex **2** and 6th protons of complex **1** would exhibit signals in the same region.

Fig. 3c shows the ^{1}H NMR spectrum of complex **1** in d_6-DMSO at 20°C. The comparison of the ^{1}H NMR spectra of **1** (Fig. 3c), **3** (Fig. 3d) and **2** (Fig. 3a) allows to attribute signals denoted in Fig. 3c by letter ''B'' to diaminocyclohexane bridge of **1**. We are still not able to assign these signals to the particular protons of a bridge. Their total intensity corresponds to four protons. The signals of the remaining six protons of the bridge may be too broad or can be masked by the intense signals of residual H_2O and DMSO. The resonance at -27 ppm ($\Delta\omega_{1/2} = 700$ Hz) belongs to 4th protons of aromatic rings of **1**.

The ^{1}H and ^{2}D NMR spectra of **1**, **2** and **3** (Fig. 3a–d) were recorded in d_6-DMSO and DMSO respectively, due to proper solubility of all complexes. These solvents are unsuitable for the epoxidation of alkenes by catalytic system **1** + PhIO, and thus the interaction of **1** with PhIO was studied in $CDCl_3$ as a solvent. The ^{1}H NMR spectrum of **1** in $CDCl_3$ at -20°C (Fig. 3e) displays an intense resonance of four *t*Bu groups at 2.6 ppm ($\Delta\omega_{1/2} = 200$ Hz), two resonances at -29.0 ppm ($\Delta\omega_{1/2} = 800$ Hz) and -32.7 ppm ($\Delta\omega_{1/2} = 800$ Hz) from nonequivalent 4th protons of **1** and signals denoted by letter B from the protons of diaminocyclohexane bridge of **1**. The signals of 6th protons of **1** are masked by that of its *t*Bu groups.

*3.2. Complex **1** + PhIO catalytic system*

Stable oxomanganese(V) complexes are few, the only examples involving the use of tetraanionic ligands to stabilize the high-valent manganese center [26,27]. Recently, nitridomanganese(V) salen complex (Salen = *N,N′*-bis(salicylidene)ethylenediamine) has been well characterized [11]. By analogy with the isoelectronic nitridomanganese(V) salen complexes and the known stable oxomanganese(V) complexes, the reactive $[(Salen)Mn^{V}=O]^{+}$is expected to be a low-spin ($S = 0$), d^2 complex. We have recorded the ^{1}H NMR spectrum of the complex $[(Salen)Mn^{V}\equiv N]$ (Salen is (*R,R*)-(−)-*N,N′*-bis(3,5-di-*tert*-butyl-salicylidene)-1,2-cyclohexanediamine) to determine the expected values of the chemical shifts for manganese(V) salen species. The model complex $[(Salen)Mn^{V}\equiv N]$ was prepared according to the procedure described in Ref. [11]. Its ^{1}H NMR spectrum (8.00 (s, 1H), 7.95 (s, 1H), 7.46 (s, 1H), 7.44 (s, 1H), 7.02 (s, 1H), 6.97 (s, 1H), 3.46– 2.03 (m, 10H), 1.49 (s, 9H), 1.45 (s, 9H), 1.28 (s, 18H), δ, $CDCl_3$, -20°C) is characteristic of diamagnetic species (Fig. 5). The line broadening observed in Fig. 5 is caused by the presence of paramagnetic admixtures formed

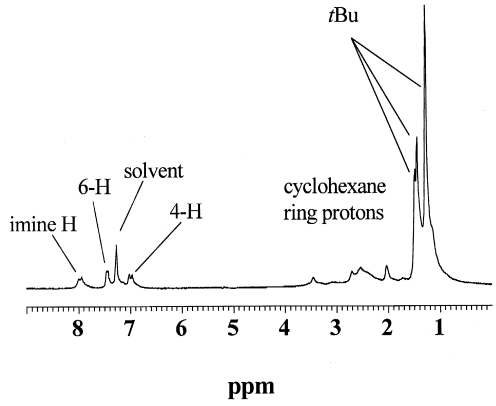

Fig. 5. ^{1}H NMR spectrum of the nitridomanganese(V) complex $[(Salen)Mn^{V}=N]$ in $CDCl_3$ (0.01 M) at -20°C.

in the course of partial decomposition of [(Salen)$Mn^{V} \equiv N$] in $CDCl_3$. The resonances at 8.00 and 7.95 ppm belong to two nonequivalent imine protons. Four signals in the region 7.5–6.9 ppm are attributed to aromatic protons. The signals at 1.49, 1.45 and 1.28 ppm belong to the protons of *t*Bu groups. The remaining signals correspond to the protons of diaminocyclohexane bridge. For comparison, the ^{1}H NMR spectrum of H_2Salen in $CDCl_3$ at -20°C displays one resonance of imine protons at 8.32 ppm, two signals from aromatic protons at 7.34 and 7.16 ppm, and two signals from *t*Bu groups at 1.42 and 1.24 ppm. The diaminocyclohexane bridge protons of H_2Salen display resonances with the field positions rather close to those in the nitridomanganese model complex.

Based on the above data, we have undertaken search of the oxomanganese(V) species in the catalytic system **1** + PhIO. For this purpose, the standard NMR tube ($d = 5$ mm) containing 0.6 ml of cooled off (-40°C) 0.02M solution of **1** in $CDCl_3$ was placed into the probe of NMR spectrometer immediately after 30 s shaking of the solution with PhIO powder (2 mg) at -40°C. The ^{1}H NMR spectrum was recorded at -20°C 5 min after onset of the reaction. Several new signals are observed in the regions 1.3–1.8 ppm (compare Fig. 6a–b). They can be attributed to the *t*Bu groups of three complexes of manganese. These complexes will be further referred to as complexes (**4**–**6**). Their resonances are denoted in Fig. 2b by corresponding symbols. Note, that H_2Salen is not liberated at the initial stage of the reaction studied. Further stirrings of the sample of Fig. 2b at low temperature give rise to the increase of the concentration of complexes (**4**–**6**) (Fig. 6c–d). The concentration of **4** exceeds those of **5** and **6** only at the initial stage of the reaction of **1** with PhIO at -20°C (Fig. 6b).

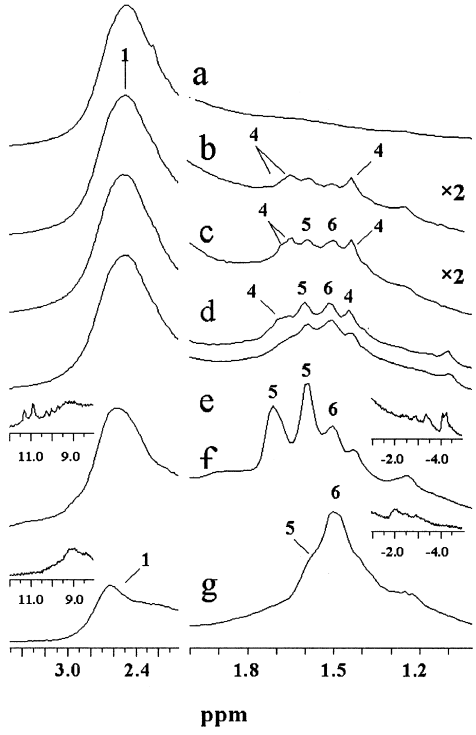

Fig. 6. ^{1}H NMR spectra of 0.02 M solution of **1** in $CDCl_3$ (0.6 ml) after subsequent stirrings with suspension of PhIO (2 mg) at -40°C: before reaction (a); first 30 s stirring (b); second 1 min stirring (c); third 1 min stirring (d); 1 min after the addition of styrene to make its concentration 0.1 M to the sample of Fig. 1d (e); sample in (d) after 2 min warming at room temperature (f); sample in (f) after stirring with additional portion of PhIO (4 mg) at 0°C (g). ^{1}H NMR spectra were recorded at -20°C (a–f) and at 0°C (g).

Complex **4** is very unstable and rapidly disappears at 0°C. The achieved concentration of complex **4** is not more than 3% of the initial concentration of **1** and those of complexes **5** and **6** can exceed 50% of the initial concentration of **1** after 3 min stirring of **1** with PhIO at 0°C. Complexes **5** and **6** are stable at −20°C and very slowly react with styrene at this temperature (characteristic time was more than 2 h, [styrene] = 0.05 M). In contrast , the addition of styrene (to make its concentration 0.1 M) to the sample of Fig. 6d at −20°C leads to the immediate drop (ca. twofold) of the concentration of complex **4** (Fig. 6e). This drop is accompanied by the appearance of the resonances of styrene oxide in the ^{1}H NMR spectrum. In the absence of styrene, concentrations of complexes (**4**–**6**) do not noticeably change during 15 min at −20°C. These data indicate that complex **4** can be reactive towards styrene. When styrene had been added to the sample containing **1** prior to the stirring with PhIO at −20°C, the immediate growth of the concentration of styrene oxide was observed by ^{1}H NMR, while formation of complexes (**4**–**6**) was almost entirely suppressed.

Complex **4** exhibits three signals of *t*Bu groups at 1.68, 1,64 and 1.42 ppm. The overall intensity of the signals at 1.68 and 1.64 ppm equals to that of the signal at 1.42 ppm. The widths of the resonances of the *t*Bu groups of complex **4** (20 Hz) are close to those of the lines of diamagnetic species (e.g., $CHCl_3$, PhI) in our particular sample. The line broadening is caused by the presence of paramagnetic Mn(III) species. The observed pattern of *t*Bu groups of complex **4** resembles that for [(Salen)$Mn^V \equiv N$] (at 1.49, 1.45 and 1.28 ppm, Fig. 5), when compare the differences in chemical shifts between the signals and their relative intensities. Unfortunately, we have not detected signals of the aromatic and imine protons of complex **4** using $COCL_3$ and CO_2CL_2 as solvents. Most probably, they are obscured by the intense resonances of PhI formed in the reaction of **1** with PhIO.

Complex **4** displays characteristic pattern of *t*Bu groups closely resembling that for a model nitridomanganese(V) salen species. It is very unstable and predominates only at the early stage of interaction of **1** with PhIO at low temperature. The effect of styrene on the concentration of **4** evidences in favor of its reactivity towards this substrate. Based on these data, complex **4** can be attributed to oxo manganese(V) intermediate [(Salen)$Mn^V = O]^+$.

Let us now discuss possible structures of complexes **5** and **6**. The concentration of complex **5** grows after warming of the sample of Fig. 6d during 2 min at room temperature (Fig. 6f). It displays two resonances of *t*Bu groups at 1.72 and 1.60 ppm, two resonances at 10.9 and 11.3 ppm, several signals in the range 4–5 ppm (not shown) and two signals at −4.1 and −4.2 ppm. The field position and width (30–80 Hz) of the observed resonances of complex **5** are typical for antiferromagnetically coupled μ−oxo dinuclear manganese(IV) species [20,21]. For these species, the ^{1}H NMR signals are much closer to their position in diamagnetic complexes, than for corresponding mononuclear Mn^{IV} and Mn^{III} complexes. Thus, the resonances at 10.9 and 11.3 ppm probably belong to aromatic protons of complex **5**. The relative concentration of complex **5** diminished and that of complex **6** increased when the sample of Fig. 6f was stirred with additional portion of PhIO (4 mg) at 0°C (Fig. 6g). The field positions and widths of the signals of complex **6** are also typical for Mn^{IV}-*O*-Mn^{IV} dimers. Probably, complexes **5** and **6** are dinuclear complexes [(Salen)Mn^{IV}-*O*-Mn^{IV}(Salen)]$^{+2}$ with different axial ligands (PhIO and Cl^-). The dimeric cation [(Salen)Mn^{IV}-*O*-Mn^{IV}(Salen)]$^{+2}$ with PhIO molecules in axial sites was detected in the catalytic system **1** + PhIO by electrospray tandem mass spectrometry [8].

The analysis of the EPR spectra of the catalytic system **1** + PhIO shows that at the early stage of interaction of **1** with PhIO at room temperature, EPR signal of the initial complex **1** at $g = 7.8$ immediately converts into an other more intensive signal at $g = 8.7$ (compare Fig. 7a and b). This conversion can be explained by the formation of the adduct (Salen)Mn^{III}(PhIO) recently observed in the catalytic system studied by electrospray tandem mass spectrometry [8]. In addition, it is seen that

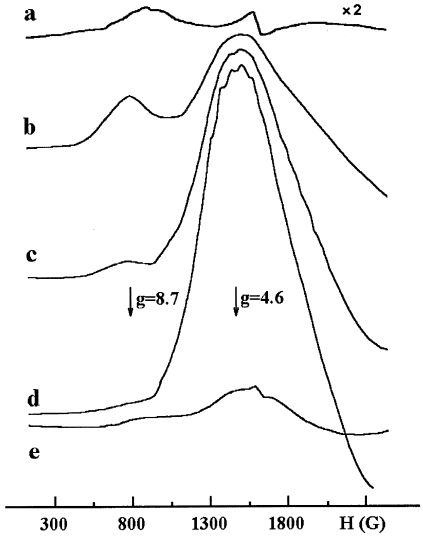

Fig. 7. X-band EPR spectra (−196°C) of 0.03 M solution of complex **1** in CH_2Cl_2 at various moments of time after stirring with 1.2 equiv. of PhIO at 20°C: before reaction (a), 20 s (b), 5 min (c), 20 min (d); X-band EPR spectrum (−196°C) of the solution of complex **1** (0.03 M) and styrene (0.4 M) in CH_2Cl_2 20 min after stirring with PhIO (1.2 equiv. with respect to **1**) at 20°C (e). Gain 1×10^5 (a), 5×10^4 (b–e).

in the course of the reaction of **1** with PhIO at room temperature, EPR signal at $g = 8.7$ diminishes and that at $g = 4.6 \pm 0.2$ characteristic for mononuclear Mn(IV) species grows (Fig. 7b–d). These still unidentified species display several broad resonances (300–800 Hz) in the range −20 to +20 ppm in the ^{1}H NMR spectrum. They are stable at room temperature and are inert towards styrene at this temperature. Probably, formation of these mononuclear Mn(IV) species leads to catalyst deactivation. When styrene is added to the solution of **1** prior to stirring with PhIO, formation of unreactive mononuclear Mn(IV) species is noticeably suppressed (compare Fig. 7d and e).

In conclusion, we demonstrate that ^{1}H NMR spectroscopy is very fruitful for the in situ characterization of oxomanganese(V) intermediate and other manganese species in the catalytic system **1** + PhIO.

*3.3. Complex **1** + m-CPBA catalytic system*

*3.3.1. Characterization of acylperoxo complex (Salen)Mn^{III}(OOCOAr)(**7**)*

One minute after the addition of one equivalent of *m*-CPBA to the 0.05 M solution of complex **1** in CH_2Cl_2 at −90°C, the intensity of its EPR signal at $g = 7.8$ sharply decreases (ca. fivefold) and the new signal of mononuclear Mn(IV) complexes at $g = 5.4 \pm 0.2$ appears (Fig. 8a–b). The latter species display ^{1}H NMR resonance of *t*Bu groups at 3.5 ppm ($\Delta\omega_{1/2} = 800$ Hz) and broad resonances at −25 ppm and at −47 ppm at −78°C (Fig.9b–c). According to ^{1}H NMR, more than 90% of the initial manganese remains in the form of Mn(III) species in the sample of Fig.8b and thus the observed signal at $g = 5.4$ corresponds only to minor conversion of the initial Mn(III) to Mn(IV). The entire conversion of Mn(III) to Mn(IV) would produce EPR signal at $g = 5.4$ five times as intense as the initial signal of complex **1** at $g = 7.8$ (cf. Fig. 8a and e). The amplification in Fig. 8e is lower than that in Fig. 8a–d by a factor of five. Thus, the observed drop of the intensity of the EPR signal of Mn(III) at $g = 7.8$ in Fig.8b is caused by the conversion of complex **1** into another complex of Mn(III), which is characterized by a lower intensity of the Mn(III) resonance. Further, it will be

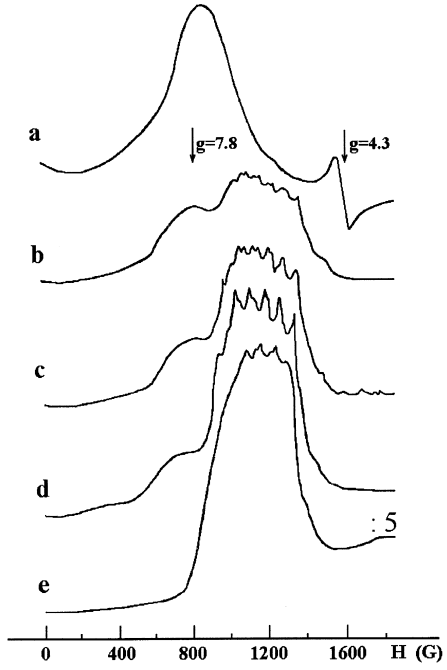

Fig. 8. X-band EPR spectra (−196 °C) of 0.05 M solution of complex **1** in CH_2Cl_2 recorded at various times after the addition of 1.2 equiv. of m-CPBA at −90°C: before reaction (a), 30 s (b), 3.5 min (c), 10 min (d); sample in (d) warmed to room temperature to complete the reaction (e). Gain 2×10^5 (a–c), 4×10^4 (e).

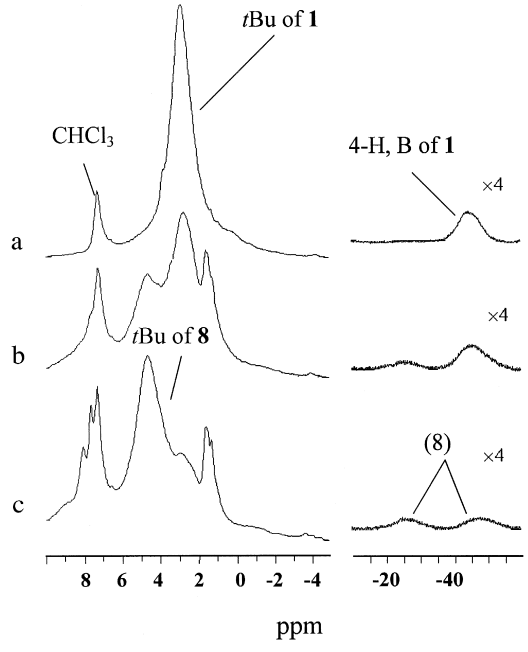

Fig. 9. ^{1}H NMR spectra of 0.02 M solution of **1** in the mixture of $CDCl_3 + CCl_4$ (1:1) at −78°C after various moments of time after addition of m-CPBA (1.2 equiv.): before reaction (a), 5 min (b), 15 min (c). The high field part of the spectra was recorded at 4-fold higher amplification. Protons of cyclohexane ring are labeled with letter B (''bridging''). Resonances at 1.41–1.59 ppm are due to the *t*Bu groups of Mn^{IV}-O-Mn^{IV} dinuclear species, a relatively narrow signal at 1.24 belongs to the *t*Bu groups of unidentified species formed in the course of Salen ligand decomposition.

referred to as complex **7**. Complex **7** is extremely unstable ($\tau_{1/2}$ = 20 min at −90°C, 3 min at −70°C and less than 0.5 min at −20°C) and rapidly and quantitatively decomposes to form metastable mononuclear Mn^{IV} species.

By analogy with the well documented formation of acylperoxo complexes via interaction of Mn(III) porphyrins with *m*-CPBA at low temperatures [28], it is natural to suppose that complex **7** is acylperoxo complex (Salen)Mn^{III}(OOCOAr). Thus, at the first stage of the interaction of complex **1** with *m*-CPBA at low temperature the acylperoxo complex Mn(III)Salen(OOCOAr) (**7**) is formed, which rapidly converts into mononuclear Mn(IV) species. Dinuclear Mn(IV) complexes like **5** and **6** have been found to form in minor concentration in the course of the interaction of **1** with *m*-CPBA.

The attempts to detect $[(Salen)Mn^{V}=O]^{+}$ intermediate in the catalytic system **1** + *m*-CPBA using ^{1}H NMR spectroscopy were unsuccessful.

EPR signal near $g = 5.4$ (Fig. 8b–e) is the superposition of the signals of at least three types of Mn(IV) species. The minor less stable species exhibit resonances with well resolved hfs from manganese $A = 75 \pm 5$ G. The major complex displays signal at $g = 5.4$ with unresolved hfs from manganese. This complex is more stable and predominates at room temperature (Fig. 8e). The similar picture was observed for the reaction of **1** with *m*-CPBA at − 70°C. However, in this case mainly one type of less stable Mn(IV) species with well resolved hfs from manganese could be observed (Fig.10).

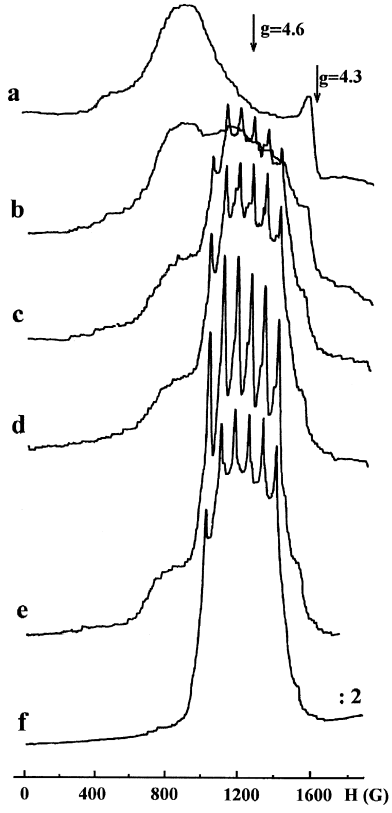

Fig. 10. X-band EPR spectra (−196°C) of 0.05 M solution of complex **1** in CH_2Cl_2 recorded at various moments of time after the addition of 1.5 equiv. of m-CPBA at −70 °C: before reaction (a); 20 s (b); 1 min (c); 2 min (d); 4.5 min (e); 20 min (f). Gain 2×10^5 (a–e), 1×10^5 (f).

Mn(IV) species with unresolved hfs from manganese very slowly decomposes back to complex **1** with characteristic time of 4h at room temperature. We have supposed that the major Mn(IV) species exhibiting EPR signal at $g = 5.4$ with unresolved hfs from manganese is Mn(IV) oxo complex formulated as (Salen)$Mn^{IV} = O(L)$ (L is an axial ligand) (complex **8**). The unstable minor Mn(IV) species with hyperfine structure from Mn (Figs. 8 and 10) is proposed to be (Salen)$Mn^{IV}(L)(L')$ complex with different L, L′.

3.3.2. Reactivity of complexes 7 and 8 towards styrene

The first-order rate constant of the conversion of the acylperoxo complex (Salen)Mn^{III} (OOCOAr) (**7**) into mononuclear Mn(IV) species (**8**) at −70°C evaluated from EPR spectra of Fig. 10 is $k_1 = 0.25 \pm 0.08$ min^{-1}. When styrene ([styrene] = 1 M) is added to the sample of Fig. 10 prior to the addition of stochiometric amount of *m*-CPBA, the observed EPR spectra markedly differ from those for the sample without styrene (compare Figs. 10 and 11). In this case the reaction (2) competes with the reaction (3) and only partial conversion of **1** to **8** is observed (Fig. 11).

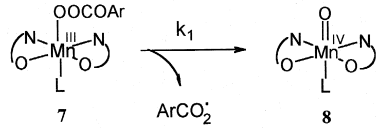

(2)

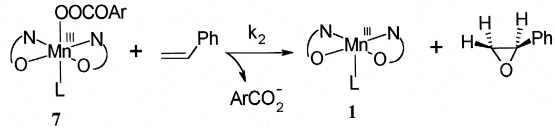

(3)

The final value of the ratio [**1**]/[**8**] is determined by the rates of the reactions (2) and (3)

$$[\mathbf{1}]/[\mathbf{8}] = k_2[S]/k_1 \tag{4}$$

where S is concentration of styrene. This value determined from the spectra of Fig. 11 is [**1**]/[**8**] = 4.5. Thus, the rate constant k_2 of the reaction of the acylperoxo complex **7** with styrene at −70°C was evaluated as 1.1 ± 0.4 M^{-1} min^{-1}. According to GS data, the products of this reaction at −70°C were styrene oxide (with 31% yield), benzaldehyde (9%) and acetophenone (8%), reaction time 2 h.

The Mn(IV) complex **8** is far less reactive towards styrene than Mn(III) acylperoxo complex **7** and reacts with styrene at noticeable rate only at high temperatures (15°C). The integral Mn(IV) EPR signal intensity obeys the first-order kinetic law, with the observed rate constant linear in the concentration of styrene. This constant was evaluated as $k = k_1 + k_2$ [styrene] where $k_1 = 0.005 \pm 0.003$ min^{-1} and $k_2 = 0.010 \pm 0.002$ l mol^{-1} min^{-1}. When **8** obtained by stirring of **1** with 1.2 equiv. of *m*-CPBA during 15 minutes at 15°C was reacted with styrene (20h at 15°C in CH_2Cl_2, aerobic conditions), the observed products were benzaldehyde (22% with respect to manganese) and styrene oxide (13%), with the consumption of styrene exceeding 120% with respect to manganese. The same reaction performed under argon atmosphere during 24 h gave only traces of benzaldehyde and styrene oxide as it was observed by GC. Note that the consumption of styrene was more than

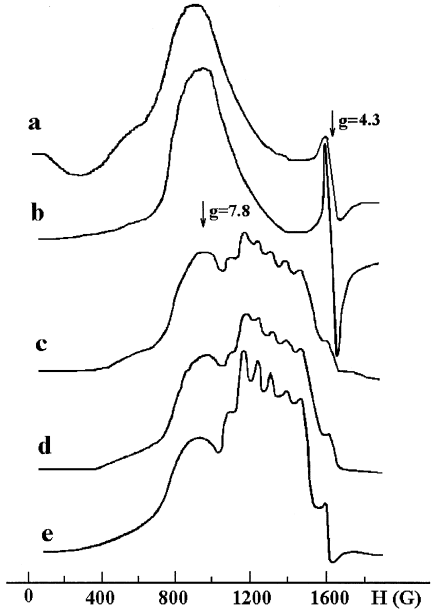

Fig. 11. X-band EPR spectra (−196°C) of 0.05 M solution of complex **1** in CH_2Cl_2 (a); after the addition of styrene (1 M) (b); sample in (b) at various moments of time after the addition of 1.2 equiv. of m-CPBA at −70°C (c–e): 20 s (c),1 min (d), 15 min (e). Gain 2×10^5 (a–e).

140% with respect to manganese. This behaviour is in agreement with the observations of Groves for the reaction of oxo complex $TMPMn^{IV}=O$ (TMP is 5,10,15,20 tetramesitylporphyrine) with *cis*-β-methylstyrene [21]. It was found that the yields of benzaldehyde, *cis*-β-methylstyrene oxide and cinnamaldehyde decreased significantly when reaction was carried out under anaerobic conditions. These arguments support our assignment of **8** to an oxo manganese(IV) intermediate.

*3.4. Complex **1** + m-CPBA + NMO catalytic system*

According to EPR data (Fig.1b–c), the addition of NMO to the sample containing **1** gives rise to the coordination of NMO to the axial coordination place of **1** and the adduct **1**-NMO is formed.

The addition of *m*-CPBA to the sample containing **1**-NMO in CH_2Cl_2 ([NMO] = 0.3 M) at −70°C gives rise to extremely fast conversion of **7**-NMO to **8**-NMO ($k_1 > 2\text{min}^{-1}$) (Fig. 12b). Thus, the rate of the conversion of the acylperoxo complex of Mn(III) into the oxo complex of Mn(IV) increases more than one order via coordination of NMO. This result agrees with the data reported for Fe(III) porphirine acylperoxo complexes. Their decomposition into Fe(IV) porphirine oxo species also increases upon axial ligation of imidazol (push effect) [29]. Complex **8**-NMO is poorly reactive towards styrene. For the catalytic system **1** + NMO + *m*-CPBA to be effective in epoxidation of styrene, the rate of the reaction of **7**-NMO with styrene at −70°C to restore **1**-NMO must be much higher than the rate of the undesirable conversion of **7**-NMO into **8**-NMO. In full agreement with this prediction, in the presence of styrene, EPR spectrum of the initial complex **1**-NMO remains unchanged after the addition of the *m*-CPBA (Fig. 12c–e). Thus, coordination of NMO dramatically magnifies (more than two orders) the rate constant k_2 of the reaction of acylperoxo complex with styrene. The yield of epoxide in this case at 0°C, 5 equiv. of NMO and reaction time 30 min was 67%, with ee 45% in agreement with literature data [6]. The axial coordination of NMO probably

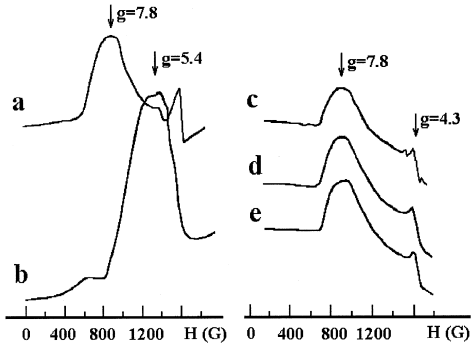

Fig. 12. X-band EPR spectra (−196°C) of 0.05 M solution of complex **1** in CH_2Cl_2 containing 0.25 M of NMO (a), 40 s after the addition of 1.2 equiv. of *m*-CPBA at − 70°C (b). X-band EPR spectra (−196°C) of 0.05 M solution of complex **1** in CH_2Cl_2 containing 0.25 M of NMO and 0.5 M of styrene recorded at various moments of time after the addition of *m*-CPBA (1.2 equiv.) at 20°C (c–e): before reaction (a), 30 s (d), 2.5 min (e). Gain 2×10^5 (a), 1×10^5 (b–e).

provides the compromise between the rate constants k_1 and k_2, to achieve high efficiency of styrene epoxidation. When Py is used instead of NMO as axial ligand, the partial conversion of the initial complex **1**-Py into **8**-Py takes place after the addition of *m*-CPBA even in the presence of styrene. Thus, the reaction of **7**-Py with styrene to restore **1**-Py is not so competitive with the conversion of **7**-Py into **8**-Py as in the case of NMO. As a result, the yield of epoxide for the catalytic system 1 + *m*-CPBA + Py (4.3 equiv.) at 0°C was low, 35% (reaction time 4 h).

The last detectable intermediate in the catalytic system **1** + *m*-CPBA is acylperoxo complex (Salen)Mn^{III}(OOCOAr) (**7**). It is very interesting to elucidate whether the Mn(III) acylperoxo intermediate directly reacts with olefins or via formation of oxomanganese(V) species. The possibility of the direct concerted reaction of acylperoxo complexes of manganese and iron with olefins is considered in the literature [30,31]. We have found that acylperoxo complex (Salen)Mn^{III}(OOCOAr) rapidly reacts with styrene at -70°C ($k_2 = 1.1 \pm 0.4$ l mol^{-1} min^{-1}), while the catalytic system **1** + PhIO exhibiting oxo manganese(V) intermediates produces styrene oxide only at temperatures higher than -30°C. Thus, the direct reaction of acylperoxo complex of Mn(III) with olefins in the catalytic system **1** + *m*-CPBA seems to be more probable.

Acknowledgements

This work was supported by Russian Foundation for Basic Research, grant 97-03-32495. We thank Dr. A.P. Sobolev for fruitful discussions.

References

[1] E.N. Jacobsen, W. Zhang, A.R. Muci, J.R. Ecker and, L. Deng, J. Am. Chem. Soc. 113 (1991) 7063.
[2] T. Katsuki, Coord. Chem. Rev. 140 (1995) 189.
[3] M. Palucki, N.S. Finney, P.J. Pospisil, M.L. Guler, T. Ishida, E.N. Jacobsen, J. Am. Chem. Soc. 120 (1998) 948.
[4] C.T. Dalton, K.M. Ryan, V.M. Wall, C. Bousquet, D.G. Gilheany, Top. Catal. 5 (1998) 75.
[5] W. Adam, R.T. Fell, V.R. Stegmann, Ch.R. Saha-Moller, J. Am. Chem. Soc. 120 (1998) 708.
[6] M. Palucki, P.J. Pospisil, W. Zhang and, E.N. Jacobsen, J. Am. Chem. Soc. 116 (1994) 9333.
[7] M. Palucki, G.J. McCormick and, E.N. Jacobsen, Tetrahedron Lett. 36 (1995) 5457.
[8] D. Feichtinger and, D.A. Plattner, Angew. Chem. Int. Ed. Engl. 36 (1997) 1718.
[9] N. Jin, J.T. Groves, J. Am. Chem. Soc. 121 (1999) 2923.

[10] K. Srinivasan, P. Michaud, J.K. Kochi, J. Am. Chem. Soc. 108 (1986) 2309.
[11] J. Du Bois, J. Hong, E.M. Carreira, M.W. Day, J. Am. Chem. Soc. 118 (1996) 915.
[12] D.S. Kemp, J. Org. Chem. 36 (1971) 202.
[13] W. Zhang and, E.N. Jacobsen, J. Org. Chem. 56 (1991) 2296.
[14] D.P. Goldberg, J. Telser, J. Krzystek, A. Garrido Montalban, L.S. Brunel, A.G.M. Barrett, B.M. Hoffman, J. Am. Chem. Soc. 119 (1997) 8722.
[15] R.L. Aurbach, P.L. Richards, Phys. Rev. B 12 (1975) 2588.
[16] H.J. Gerritsen, E.S. Sabisky, Phys. Rev. 132 (1963) 1507.
[17] S.L. Dexheimer, J.W. Gohdes, M.K. Chan, K.S. Hagen, W.H. Armstrong, M.P. Klein, J. Am. Chem. Soc. 111 (1989) 8923.
[18] S. Pal, P. Ghosh, A. Chakravorty, Inorg. Chem. 24 (1985) 3704.
[19] D.P. Kessissglou, W.M. Butler, V.L. Pecoraro, J. Chem. Soc. Chem. Commun. (1986) 1253.
[20] J.A. Smegal, C.L. Hill, J. Am. Chem. Soc. 105 (1983) 3515.
[21] J.T. Groves, M.K. Stern, J. Am. Chem. Soc. 110 (1988) 8628.
[22] B. Mabad, J.-P. Tuchagues, Y.T. Hwang, D.N. Hendrickson, J. Am. Chem. Soc. 107 (1985) 2801.
[23] G.C. Dismukes, J.E. Sheats, J.A. Smegal, J. Am. Chem. Soc. 109 (1987) 7202.
[24] T.J. Swift, in: G.N Lamar, W.D. Horrocks, R.H. Holm (Eds.), NMR Paramagn. Mol., Academic Press, New York, 1973, p. 53.
[25] J.A. Bonadies, M.J. Maroney, V.L. Pecoraro, Inorg. Chem. 28 (1989) 2044.
[26] T.J. Collins, R.D. Powell, R.D. Powell, C. Slebodnick, E.S. Uffelman, J. Am. Chem. Soc. 112 (1990) 899.
[27] T.J. Collins, S.W. Gordon-Wylie, J. Am. Chem. Soc. 111 (1989) 4511.
[28] J.T. Groves, Y. Watanabe, Inorg. Chem. 25 (1986) 4808.
[29] K. Yamaguchi, Y. Watanabe, I. Morishima, J. Am. Chem. Soc. 115 (1993) 4058.
[30] T. Yamada, K. Imagawa, T. Nagata, T. Mukaiyama, Bull. Chem. Soc. Jpn. 67 (1994) 2248.
[31] K. Kamaraj, D.J. Bandyopadhyay, J. Am. Chem. Soc. 119 (1997) 8099.